2004 IEEE 5th Workshop on Signal Processing Advances in Wireless Communications

MIMO Space-Time Block Coded Receivers over Frequency Selective Fading Channels

Waleed M. Younis and Ali. H. Sayed[1]
Electrical Engineering Department
University of California
Los Angeles, CA 90095
Email: {waleed, sayed}@ee.ucla.edu

Abstract — **We develop an adaptive receiver for multiple-input multiple-output (MIMO) frequency selective channels that employ space-time block-coded transmissions with cyclic prefixing. The receiver performs both interference suppression and equalization for multi-user transmissions. The structure of the space-time code is exploited to show that the receiver can be implemented on a per-frequency-bin basis rather than on a block-by-block basis. The adaptation scheme requires solving N independent problems each of complexity $\mathcal{O}(M^2)$ per block iteration, where M is the number of users and N is the block size.**

I. Introduction

Multiple-input multiple-output (MIMO) architectures offer attractive schemes that could improve the communications performance and reliability over wideband channels [1]. Using multiple antennas at both the transmitter and receiver sides adds diversity to the channel and enables transmission at higher data rates. Some of the factors that typically affect performance and complexity are the number of users, the number of transmit and receive antennas, channel memory, and multi-path fading conditions. Among the promising encoding schemes for MIMO wireless systems are space-time block codes (STBC) (e.g., [2], [3]). They provide full diversity gains and achieve good performance with simple receiver structures, especially over flat fading channels. In [4] and [5] block extensions of these codes that exploit multipath diversity over frequency selective fading channels are discussed.

The scheme of [5] adds a cyclic prefix to each block and a single-carrier frequency-domain equalizer (SC-FDE) is then used to decode the data. This scheme is similar to orthogonal frequency division multiplexing (OFDM) except that it uses a single carrier and the decisions are made in the time domain. Moreover, it is less sensitive to carrier frequency offset and non-linear distortion than OFDM.

It was shown in [6] that the SC-FDE STBC scheme can be used to increase system capacity by allowing two co-channel users to transmit simultaneously in a TDMA environment and by employing a zero forcing interference cancellation and equalization scheme at the receiver. This scheme was extended to the multi-user case in [7] and, in addition, an implementation was developed that delivers recursive least-squares (RLS) performance at least mean-squares (LMS) complexity by exploiting the code structure. One advantage of the adaptive receiver structure is that it does not require channel state information (CSI) at the receiver [8]. More recently, it was shown in [9] that for the case of two users, joint MMSE interference suppression and equalization can be implemented on a per-frequency-bin basis rather than on a block-by-block basis.

In this paper, we show that such a symbol level implementation is also possible for a MIMO system consisting of M users with two transmit antennas each and M receive antennas. In particular, we use this fact to reduce the computational complexity of the adaptive receivers of [7],[8] to N independent problems, with each one requiring $\mathcal{O}(M^2)$ operations per block iteration where M is the number of users and N is the block size.

II. Problem Formulation

With M users, each equipped with two antennas, we can use M receive antennas to decouple all users and increase the system capacity. The block diagram of the system is shown in Figure 1. The explanation for the notation that is used for the data and channel matrices throughout the paper is shown in Figure 2. For each user, data are transmitted from its two antennas in blocks of length N according to the space-time coding scheme indicated in Figure 3. Denote the n-th symbol of the k-th transmitted block from antenna j of user i by $\mathbf{x}_{k,j}^{(i)}(n)$. At times $k = 0, 2, 4, \cdots$, the blocks $\mathbf{x}_{k,1}^{(i)}(n)$ and $\mathbf{x}_{k,2}^{(i)}(n)$ $(0 \le n \le N-1)$ are generated by an information source according to the rule [5]:

$$\mathbf{x}_{k+1,1}^{(i)}(n) = -\mathbf{x}_{k,2}^{*(i)}\left((-n)_N\right), \quad \mathbf{x}_{k+1,2}^{(i)}(n) = \mathbf{x}_{k,1}^{*(i)}\left((-n)_N\right) \quad (1)$$

where each data vector $\mathbf{x}_{k,j}^{(i)}$ has a covariance matrix equal to $\sigma_x^2 \mathbf{I}_N$, and where $(\cdot)^*$ and $(\cdot)_N$ denote complex conjugation and modulo-N operations, respectively. In addition, a cyclic prefix (CP) of length ν is added to each transmitted block to eliminate inter-block interference (IBI) and to make all channel matrices *circulant*. Here, ν denotes the longest channel memory between the transmit antennas and the receive antennas. With

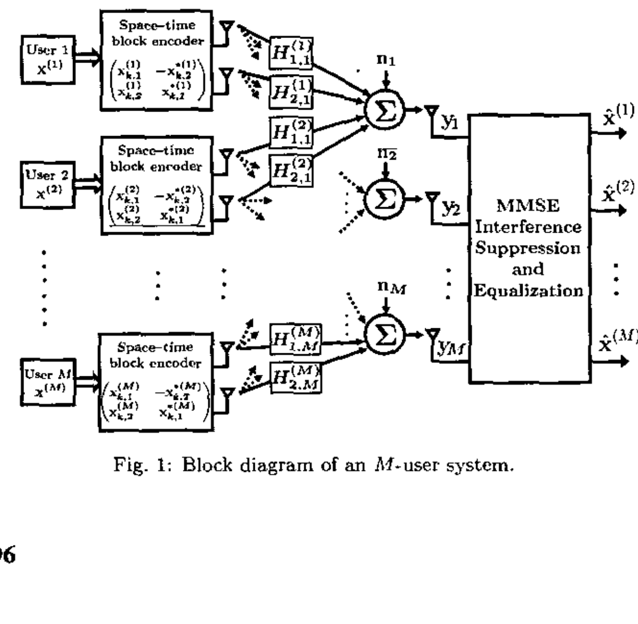

Fig. 1: Block diagram of an M-user system.

[1] This work was partially supported by NSF grants CCR-0208573 and ECS-0401188.

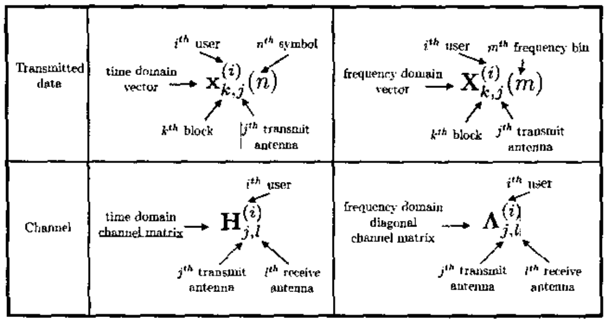

Fig. 2: Notation used for data blocks and channel matrices.

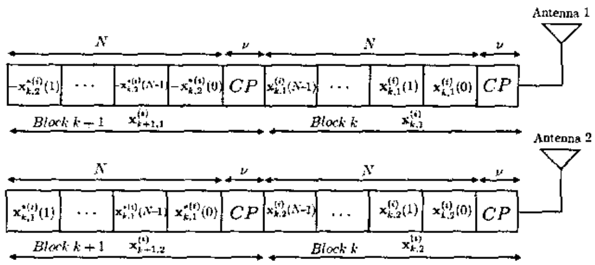

Fig. 3: Block format for SC FDE–STBC transmission scheme.

two transmit antennas per user and M receive antennas, and assuming all channels are fixed over two consecutive blocks, the received blocks k and $k+1$ at the l–th receive antenna, in the presence of additive white noise, are described by

$$\mathbf{y}_{q,l} = \sum_{i=1}^{M} \left(\mathbf{H}_{1,l}^{(i)} \mathbf{x}_{q,1}^{(i)} + \mathbf{H}_{2,l}^{(i)} \mathbf{x}_{q,2}^{(i)} \right) + \mathbf{n}_{q,l}, \; q = k, k+1 \quad (2)$$

where $\mathbf{n}_{k,l}$ and $\mathbf{n}_{k+1,l}$ are the noise vectors for the received blocks k and $k+1$, respectively, with covariance matrix $\sigma_n^2 \mathbf{I}_N$, and $\mathbf{H}_{1,l}^{(i)}$ and $\mathbf{H}_{2,l}^{(i)}$ are the *circulant* channel matrices from the first and second transmit antennas of the i–th user, respectively, to the l–th receive antenna. Applying the DFT matrix $\mathbf{Q}$ to $\mathbf{y}_{q,l}$ in (2), we get a relation in terms of frequency–transformed variables:

$$\mathbf{Y}_{q,l} \triangleq \mathbf{Q}\mathbf{y}_{q,l} = \sum_{i=1}^{M} \left(\mathbf{\Lambda}_{1,l}^{(i)} \mathbf{X}_{q,1}^{(i)} + \mathbf{\Lambda}_{2,l}^{(i)} \mathbf{X}_{q,2}^{(i)} \right) + \mathbf{N}_{q,l}, \; q = k, k+1 \quad (3)$$

where $\mathbf{X} = \mathbf{Q}\mathbf{x}$, $\mathbf{N} = \mathbf{Q}\mathbf{n}$, and $\mathbf{\Lambda}_{1,l}^{(i)}$ and $\mathbf{\Lambda}_{2,l}^{(i)}$ are diagonal matrices given by $\mathbf{\Lambda}_{1,l}^{(i)} = \mathbf{Q}\mathbf{H}_{1,l}^{(i)}\mathbf{Q}^*$ and $\mathbf{\Lambda}_{2,l}^{(i)} = \mathbf{Q}\mathbf{H}_{2,l}^{(i)}\mathbf{Q}^*$, respectively. Using the encoding rule (1) and properties of the DFT [10], we have that

$$\mathbf{X}_{k+1,1}^{(i)}(m) = -\mathbf{X}_{k,2}^{*(i)}(m), \; \mathbf{X}_{k+1,2}^{(i)}(m) = \mathbf{X}_{k,1}^{*(i)}(m) \quad (4)$$

for $m = 0, 1, \cdots, N-1$ and $k = 0, 2, 4, \cdots$. Combining (3) and (4), we arrive at the linear relation given by (5), where $\bar{(\cdot)}$ denotes complex conjugation of the entries of the vector. Equation (5) tells us how the entries of the transformed vectors at the l–th receive antenna, $\{\mathbf{Y}_{k,l}, \mathbf{Y}_{k+1,l}\}$, are related to the entries of the transformed transmitted blocks $\{\mathbf{X}_{k,1}^{(i)}, \mathbf{X}_{k,2}^{(i)}\}$ from the two antennas of the i–th user. We can reorder the entries of (5) to obtain (6). Let

$$\mathbf{Y}_l(m) = \begin{pmatrix} \mathbf{Y}_{k,l}(m) \\ \bar{\mathbf{Y}}_{k+1,l}(m) \end{pmatrix}, \; \mathbf{\Lambda}_l^{(i)}(m) = \begin{pmatrix} \mathbf{\Lambda}_{1,l}^{(i)}(m) & \mathbf{\Lambda}_{2,l}^{*(i)}(m) \\ \mathbf{\Lambda}_{2,l}^{*(i)}(m) & -\mathbf{\Lambda}_{1,l}^{*(i)}(m) \end{pmatrix}$$

and

$$\mathbf{X}^{(i)}(m) = \begin{pmatrix} \mathbf{X}_{k,1}^{(i)}(m) \\ \mathbf{X}_{k,2}^{(i)}(m) \end{pmatrix}, \; \mathbf{N}_l(m) = \begin{pmatrix} \mathbf{N}_{k,l}(m) \\ \bar{\mathbf{N}}_{k+1,l}(m) \end{pmatrix}$$

Then the m–th entry of the received vectors from all receive antennas can be written as (7). We can now concatenate the received vectors $\mathbf{Y}(m)$ for $m = 0, \cdots, N-1$ to get a vector $\mathbf{Y}$ that contains the samples of blocks k and $k+1$ from all receive antennas:

$$\mathbf{Y} \triangleq \underbrace{\begin{pmatrix} \mathbf{Y}(0) \\ \mathbf{Y}(1) \\ \vdots \\ \mathbf{Y}(N-1) \end{pmatrix}}_{2MN \times 1} = \underbrace{\begin{pmatrix} \mathbf{\Lambda}(0) & & & \\ & \mathbf{\Lambda}(1) & & \\ & & \ddots & \\ & & & \mathbf{\Lambda}(N-1) \end{pmatrix}}_{2MN \times 2MN} \underbrace{\begin{pmatrix} \mathbf{X}(0) \\ \mathbf{X}(1) \\ \vdots \\ \mathbf{X}(N-1) \end{pmatrix}}_{2MN \times 1}$$

$$+ \underbrace{\begin{pmatrix} \mathbf{N}(0) \\ \mathbf{N}(1) \\ \vdots \\ \mathbf{N}(N-1) \end{pmatrix}}_{2MN \times 1} \triangleq \mathbf{\Lambda}\mathbf{X} + \mathbf{N} \quad (8)$$

The minimum mean square error (MMSE) estimator of $\mathbf{X}$ given $\mathbf{Y}$ is now seen to be [11]:

$$\hat{\mathbf{X}} = \left(\mathbf{\Lambda}^* \mathbf{\Lambda} + \frac{1}{\mathrm{SNR}} \mathbf{I}_{2MN} \right)^{-1} \mathbf{\Lambda}^* \mathbf{Y}$$

$$= \begin{pmatrix} \mathbf{\Lambda}^*(0)\mathbf{\Lambda}(0) + \frac{1}{\mathrm{SNR}}\mathbf{I}_{2M} & & \\ & \ddots & \\ & & \mathbf{\Lambda}^*(N-1)\mathbf{\Lambda}(N-1) + \frac{1}{\mathrm{SNR}}\mathbf{I}_{2M} \end{pmatrix}^{-1} \mathbf{\Lambda}^* \mathbf{Y} \quad (9)$$

where $\mathbf{I}_{2MN}$ and $\mathbf{I}_{2M}$ are the $2MN \times 2MN$ and $2M \times 2M$ identity matrices, respectively. By examining the structure of (9), we see that the MMSE estimator can be evaluated on a per-frequency-bin basis since (9) decouples for $m = 0, \cdots, N-1$. Then, the minimum mean square error (MMSE) estimator of $\mathbf{X}(m)$ given $\mathbf{Y}(m)$ is given by

$$\begin{aligned} \hat{\mathbf{X}}(m) &= \mathbf{\Gamma}^{-1}(m)\mathbf{\Lambda}^*(m)\mathbf{Y}(m) \\ &= \left(\mathbf{\Lambda}^*(m)\mathbf{\Lambda}(m) + \frac{1}{\mathrm{SNR}}\mathbf{I}_{2M} \right)^{-1} \mathbf{\Lambda}^*(m)\mathbf{Y}(m) \quad (10) \end{aligned}$$

for $m = 0, \cdots, N-1$. The matrix structure of $\mathbf{\Lambda}(m)$ in (10) can be exploited to simplify the matrix inverse needed for the MMSE solution. The subblocks of each $\mathbf{\Lambda}(m)$ in (6) (namely, $\mathbf{\Lambda}_l^{(i)}(m)$ for $l, i = 1, \cdots, M$) are 2×2 *Alamouti* matrices [7], [8]. By examining the structure of (7), (8), and the MMSE solution of (10), we see that the system decouples into N parallel subsystems, with each subsystem consisting of M users and with each user using the standard 2×2 Alamouti scheme for flat fading channels [2]. This means that the complexity of the receiver becomes similar to that of the receiver of an Alamouti STBC over flat fading channel. We note the following properties of Alamouti matrices:

- The sum, difference, or product of two Alamouti matrices is an Alamouti matrix.
- The inverse of an Alamouti matrix is Alamouti.
- The inverse of a block matrix with Alamouti subblocks is a block matrix with Alamouti subblocks.

Using these properties we see that $\mathbf{\Gamma}(m)$ has a block structure with Alamouti subblocks. Therefore, $\mathbf{\Gamma}^{-1}(m)$ is also a block matrix with Alamouti subblocks. The matrix inverse can be easily computed using successive block matrix inversions. The computational complexity of the MMSE receiver is shown in Figure 4 in comparison to the joint zero-forcing interference canceller / single-user MMSE receiver in [8]. Figure 4 shows that the MMSE receiver enjoys a lower complexity than the receiver of [8]. Moreover, it is shown in Section IV that it has a better performance.

$$
\left(\begin{array}{c}\mathbf{Y}_{k,l}\\ \hline \bar{\mathbf{Y}}_{k+1,l}\end{array}\right)=\left(\begin{array}{c}\mathbf{Y}_{k,l}(0)\\ \vdots\\ \mathbf{Y}_{k,l}(N-1)\\ \hline \bar{\mathbf{Y}}_{k+1,l}(0)\\ \vdots\\ \bar{\mathbf{Y}}_{k+1,l}(N-1)\end{array}\right)=\sum_{i=1}^{M}\left(\begin{array}{ccc|ccc}\mathbf{\Lambda}_{1,l}^{(i)}(0) & & & \mathbf{\Lambda}_{2,0}^{(i)}(1) & & \\ & \ddots & & & \ddots & \\ & & \mathbf{\Lambda}_{1,l}^{(i)}(N-1) & & & \mathbf{\Lambda}_{2,l}^{(i)}(N-1)\\ \hline \mathbf{\Lambda}_{2,l}^{*(i)}(0) & & & -\mathbf{\Lambda}_{1,l}^{*(i)}(0) & & \\ & \ddots & & & \ddots & \\ & & \mathbf{\Lambda}_{2,l}^{*(i)}(N-1) & & & -\mathbf{\Lambda}_{1,l}^{*(i)}(N-1)\end{array}\right)\left(\begin{array}{c}\mathbf{X}_{k,1}^{(i)}(0)\\ \vdots\\ \mathbf{X}_{k,1}^{(i)}(N-1)\\ \hline \mathbf{X}_{k,2}^{(i)}(0)\\ \vdots\\ \mathbf{X}_{k,2}^{(i)}(N-1)\end{array}\right)+\left(\begin{array}{c}\mathbf{N}_{k,l}(0)\\ \vdots\\ \mathbf{N}_{k,l}(N-1)\\ \hline \bar{\mathbf{N}}_{k+1,l}(0)\\ \vdots\\ \bar{\mathbf{N}}_{k+1,l}(N-1)\end{array}\right) \tag{5}
$$

$$
\mathbf{Y}_l \triangleq \left(\begin{array}{c}\mathbf{Y}_{k,l}(0)\\ \bar{\mathbf{Y}}_{k+1,l}(0)\\ \hline \vdots\\ \hline \mathbf{Y}_{k,l}(N-1)\\ \bar{\mathbf{Y}}_{k+1,l}(N-1)\end{array}\right)=\sum_{i=1}^{M}\begin{pmatrix}\mathbf{\Lambda}_{1,l}^{(i)}(0) & \mathbf{\Lambda}_{2,l}^{*(i)}(0) & & & \\ \mathbf{\Lambda}_{2,l}^{*(i)}(0) & -\mathbf{\Lambda}_{1,l}^{*(i)}(0) & & & \\ & & \ddots & & \\ & & & \mathbf{\Lambda}_{1,l}^{(i)}(N-1) & \mathbf{\Lambda}_{2,l}^{*(i)}(N-1)\\ & & & \mathbf{\Lambda}_{2,l}^{*(i)}(N-1) & -\mathbf{\Lambda}_{1,l}^{*(i)}(N-1)\end{pmatrix}\left(\begin{array}{c}\mathbf{X}_{k,1}^{(i)}(0)\\ \mathbf{X}_{k,2}^{(i)}(0)\\ \hline \vdots\\ \hline \mathbf{X}_{k,1}^{(i)}(N-1)\\ \mathbf{X}_{k,2}^{(i)}(N-1)\end{array}\right)+\left(\begin{array}{c}\mathbf{N}_{k,l}(0)\\ \bar{\mathbf{N}}_{k+1,l}(0)\\ \hline \vdots\\ \hline \mathbf{N}_{k,l}(N-1)\\ \bar{\mathbf{N}}_{k+1,l}(N-1)\end{array}\right) \tag{6}
$$

$$
\begin{aligned}
\mathbf{Y}(m) \triangleq \underbrace{\begin{pmatrix}\mathbf{Y}_1(m)\\ \mathbf{Y}_2(m)\\ \vdots\\ \mathbf{Y}_M(m)\end{pmatrix}}_{2M\times 1} &= \underbrace{\begin{pmatrix}\mathbf{\Lambda}_1^{(1)}(m) & \mathbf{\Lambda}_1^{(2)}(m) & \dots & \mathbf{\Lambda}_1^{(M)}(m)\\ \mathbf{\Lambda}_2^{(1)}(m) & \mathbf{\Lambda}_2^{(2)}(m) & \dots & \mathbf{\Lambda}_2^{(M)}(m)\\ \vdots & \vdots & \ddots & \vdots\\ \mathbf{\Lambda}_M^{(1)}(m) & \mathbf{\Lambda}_M^{(2)}(m) & \dots & \mathbf{\Lambda}_M^{(M)}(m)\end{pmatrix}}_{2M\times 2M}\underbrace{\begin{pmatrix}\mathbf{X}^{(1)}(m)\\ \mathbf{X}^{(2)}(m)\\ \vdots\\ \mathbf{X}^{(M)}(m)\end{pmatrix}}_{2M\times 1}+\underbrace{\begin{pmatrix}\mathbf{N}_1(m)\\ \mathbf{N}_2(m)\\ \vdots\\ \mathbf{N}_M(m)\end{pmatrix}}_{2M\times 1}\\
&\triangleq \mathbf{\Lambda}(m)\mathbf{X}(m)+\mathbf{N}(m)
\end{aligned} \tag{7}
$$

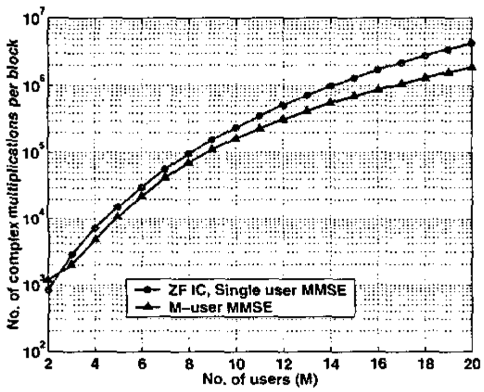

Fig. 4: Number of complex multiplications required per 2-blocks for $N = 32$.

III. Adaptive Equalization Scheme

By inspecting the structure of the MMSE equalizer and interference canceller (10), we find that the mapping from the $\{\mathbf{Y}(m)\}$ to the $\{\hat{\mathbf{X}}(m)\}$ has the following form:

$$
\begin{pmatrix}\hat{\mathbf{X}}^{(1)}(m)\\ \hat{\mathbf{X}}^{(2)}(m)\\ \vdots\\ \hat{\mathbf{X}}^{(M)}(m)\end{pmatrix}=\begin{pmatrix}\mathbf{A}_1^{(1)}(m) & \mathbf{A}_1^{(2)}(m) & \dots & \mathbf{A}_1^{(M)}(m)\\ \mathbf{A}_2^{(1)}(m) & \mathbf{A}_2^{(2)}(m) & \dots & \mathbf{A}_2^{(M)}(m)\\ \vdots & \vdots & \ddots & \vdots\\ \mathbf{A}_M^{(1)}(m) & \mathbf{A}_M^{(2)}(m) & \dots & \mathbf{A}_M^{(M)}(m)\end{pmatrix}\begin{pmatrix}\mathbf{Y}_1(m)\\ \mathbf{Y}_2(m)\\ \vdots\\ \mathbf{Y}_M(m)\end{pmatrix} \tag{11}
$$

where each $\mathbf{A}_l^{(i)}(m), l, i = 1, \cdots, M$, has an Alamouti structure. The explicit knowledge of the entries of these matrices is not needed for the development of the adaptive solution. Denote the entries of each 2×2 submatrix $\mathbf{A}_l^{(i)}(m)$ by:

$$
\mathbf{A}_l^{(i)}(m)=\begin{pmatrix}w_{1,l}^{(i)}(m) & w_{2,l}^{(i)}(m)\\ w_{2,l}^{*(i)}(m) & -w_{2,l}^{*(i)}(m)\end{pmatrix} \tag{12}
$$

Equation (11) then gives

$$
\begin{aligned}
\begin{pmatrix}\hat{\mathbf{X}}_{k,1}^{(i)}(m)\\ \hat{\mathbf{X}}_{k,2}^{(i)}(m)\end{pmatrix} &= \sum_{l=1}^{M}\begin{pmatrix}\mathbf{Y}_{k,l}(m) & \bar{\mathbf{Y}}_{k+1,l}(m)\\ -\mathbf{Y}_{k+1,l}(m) & \bar{\mathbf{Y}}_{k,l}(m)\end{pmatrix}\begin{pmatrix}w_{1,l}^{(i)}(m)\\ w_{2,l}^{(i)}(m)\end{pmatrix}\\
&\triangleq \sum_{l=1}^{M}\mathbf{U}_{k,l}(m)\mathcal{W}_l^{(i)}(m) \triangleq \mathcal{U}_k(m)\mathcal{W}^{(i)}(m)
\end{aligned} \tag{13}
$$

for $i = 1, \cdots, M$, and $m = 0, \cdots, N-1$ and where $\mathcal{U}_k(m) = (\mathbf{U}_{k,1}(m) \;\; \dots \;\; \mathbf{U}_{k,M}(m))$ is a $2 \times 2M$ matrix and $\mathcal{W}^{(i)}(m)$ is a $2M \times 1$ vector given by

$$
\mathcal{W}^{(i)}(m)=\begin{pmatrix}\mathcal{W}_1^{(i)}(m)\\ \vdots\\ \mathcal{W}_M^{(i)}(m)\end{pmatrix}
$$

The equalizer coefficients $\mathcal{W}^{(i)}(m)$ can be computed alternatively in an adaptive manner. For instance, the RLS algorithm can be used for this purpose:

$$
\begin{aligned}
\mathcal{W}_{k+2}^{(i)}(m) &= \mathcal{W}_k^{(i)}(m)+\lambda^{-1}\mathcal{P}_k(m)\mathcal{U}_{k+2}^{*}(m)\mathbf{\Pi}_{k+2}(m)\\
&\quad\times\left[\mathbf{D}_{k+2}^{(i)}(m)-\mathcal{U}_{k+2}(m)\mathcal{W}_k^{(i)}(m)\right]
\end{aligned} \tag{14}
$$

where $\mathcal{P}_k(m)$ and $\mathbf{\Pi}_k(m)$ are updated as follows:

$$
\begin{aligned}
\mathcal{P}_{k+2}(m) &= \lambda^{-1}\left[\mathcal{P}_k(m)-\lambda^{-1}\mathcal{P}_k(m)\mathcal{U}_{k+2}^{*}(m)\right.\\
&\qquad\left.\times\mathbf{\Pi}_{k+2}^{*}(m)\mathcal{U}_{k+2}(m)\mathcal{P}_k(m)^{*}\right]\\
\mathbf{\Pi}_{k+2}(m) &= \left(\mathbf{I}_2+\lambda^{-1}\mathcal{U}_{k+2}(m)\mathcal{P}_k(m)\mathcal{U}_{k+2}^{*}(m)\right)^{-1}
\end{aligned}
$$

The quantities $\{\mathcal{W}_k^{(i)}(m), \mathbf{\Pi}_k(m)\}$ are updated over k for each $m = 0, \cdots, N-1$. The initial conditions are $\mathcal{W}_0^{i}(m) = \mathbf{0}$ and $\mathcal{P}_0(m) = \delta\mathbf{I}_{2M}$, where δ is a large number. Moreover, $\mathbf{D}_{k+2}^{i}(m)$

is the desired response vector given by:

$$\mathbf{D}_{k+2}^{(i)}(m) = \begin{cases} \begin{pmatrix} \mathbf{X}_{k+2,1}^{(i)}(m) \\ \bar{\mathbf{X}}_{k+2,2}^{(i)}(m) \end{pmatrix} & \text{for training} \\ \begin{pmatrix} \check{\mathbf{X}}_{k+2,1}^{(i)}(m) \\ \bar{\check{\mathbf{X}}}_{k+2,2}^{(i)}(m) \end{pmatrix} & \text{for tracking} \end{cases} \tag{15}$$

with $\check{\mathbf{X}}_{k+2,1}^{(i)}(m)$ and $\check{\mathbf{X}}_{k+2,2}^{(i)}(m)$ being the m–th DFT coefficients of the first and second blocks of the estimates $\check{\mathbf{x}}_{k+2,1}^{(i)}$ and $\check{\mathbf{x}}_{k+2,2}^{(i)}$, respectively. The block diagram of the adaptive receiver is shown in Figure 5. The received signals from both antennas are transformed to the frequency domain using DFT. Then the m–th DFT coefficients of the l–th receive antenna are combined together to generate the data matrix $\mathbf{U}_{k,l}(m)$. The m–th DFT coefficients from all receive antennas are used to form $\mathcal{U}_k(m)$. Each $\mathcal{U}_k(m)$ is applied to M adaptive filters to form the frequency domain estimates for the M users' m–th DFT coefficients $\hat{\mathbf{X}}^{(1)}(m), \cdots, \hat{\mathbf{X}}^{(M)}(m)$. The N DFT coefficients of each user are collected in a single vector and transformed back to the time domain using IDFT and decision devices are used to generate the receiver outputs. At the beginning, known training data blocks are used to generate the desired response vector that is used to update the filter coefficients. This is the training mode of operation. Upon convergence of the adaptive algorithm, the receiver switches to a decision–directed mode where time domain estimates are converted back to the frequency domain then compared to the corresponding receiver outputs to generate the error and the desired response vectors. The desired response vectors are used to update the corresponding coefficients according to the RLS algorithm. We now proceed in a manner similar to [8] to show how the computational complexity of the adaptive solution can be reduced by exploiting the STBC structure. It is straightforward to show that the matrices $\mathcal{P}_k(m)$ and $\mathbf{\Pi}_k(m)$ will have the following structure:

$$\mathcal{P}_k(m) = \underbrace{\begin{pmatrix} \mathbf{P}_{k,1}^{(1)}(m) & \dots & \mathbf{P}_{k,M}^{(1)}(m) \\ \vdots & \ddots & \vdots \\ \mathbf{P}_{k,1}^{(M)}(m) & \dots & \mathbf{P}_{k,M}^{(M)}(m) \end{pmatrix}}_{2M \times 2M} \tag{16}$$

and

$$\mathbf{\Pi}_k(m) = \underbrace{\begin{pmatrix} \pi_k^{(1)}(m) & \pi_k^{(2)}(m) \\ -\pi_k^{*(2)}(m) & \pi_k^{*(1)}(m) \end{pmatrix}}_{2\times 2} \tag{17}$$

where $\mathbf{\Pi}_k(m)$ and each $\mathbf{P}_{k,l}^{(i)}(m)$ are 2×2 Alamouti. Table 1 shows how we exploit the structures of $\mathbf{\Pi}_k(m)$ and $\mathcal{P}_k(m)$ to update the entries of the latter.

The adaptive algorithm in Table 1 requires $N\mathcal{O}(M^2)$ complex multiplications per 2–block iterations whereas the full RLS solution that does not exploit the STBC structure requires $\mathcal{O}(N^3M^2)$ complex multiplications per 2–block iterations.

IV. Simulation Results

We start with the scenario where an MMSE equalizer is used. The system has M users, each equipped with two transmit antennas. The number of receive antennas is equal to the number of users. The channels from each transmit antenna to each receive antenna are assumed to be independent. A Typical Urban (TU) channel model with overall channel impulse response memory ν equals to 3 is considered for all channels. Moreover, a linearized GMSK transmit pulse shape is used. The data bits of each user are mapped into AN 8-PSK signal constellation and they are grouped into blocks of 32 symbols. A cyclic prefix is added to each block by copying the first ν symbols after the last symbol of the same block. The processed blocks are transmitted at a symbol rate equal to 271 KSymbols/sec. The signal to noise ratios of all users at the receiver are assumed to be equal. To simulate the performance of the receiver, We assume perfect knowledge of the channel impulse response at the receiver. We use the channel coefficients to compute the equalizer coefficients using (10).

Tab. 1: Adaptation algorithm for M users.

Set the initial conditions to

$$\mathcal{W}_0^{(i)}(m) = 0 \qquad \text{and} \qquad \mathcal{P}_0(m) = \delta \mathbf{I}_{2M}$$

where δ is a large number. Starting from $k = 0$, and for $m = 0, \cdots, N-1$, update $\mathcal{P}_k(m)$ as follows:

1. Compute the entries of $\mathbf{\Pi}_{k+2}(m)$

$$\mathbf{\Pi}_{k+2}(m) = \left(\mathbf{I}_2 + \lambda^{-1} \sum_{l=1}^{M}\sum_{i=1}^{M} \mathbf{U}_{k,i}(m)\mathbf{P}_{k,l}^{(i)}(m)\mathbf{U}_{k,l}^{*}(m)\right)^{-1}$$

2. Let $\mathbf{\Phi}_k(m) = \mathcal{U}_{k+2}^{*}(m)\mathbf{\Pi}_{k+2}(m)\mathcal{U}_{k+2}(m)$. It has a structure similar to $\mathcal{P}_k(m)$. Then the 2×2 Alamouti matrices $\mathbf{\Phi}_{k,l}^{(i)}(m)$, $i, l = 1, \cdots, M$, are given by

$$\mathbf{\Phi}_{k,l}^{(i)}(m) = \mathbf{U}_{k+2,i}^{*}(m)\mathbf{\Pi}_{k+2}(m)\mathbf{U}_{k+2,l}(m)$$

3. Update $\mathbf{P}_{ij}(k+2)$, the 2×2 block entries of $\mathcal{P}_{k+2}(m)$, as

$$\mathbf{P}_{k+2,l}^{(i)}(m) = \lambda^{-1}\mathbf{P}_{k,l}^{(i)}(m) - \lambda^{-2}\sum_{q=1}^{M}\sum_{j=1}^{M} \mathbf{P}_{k,j}^{(i)}(m)\mathbf{\Phi}_{k,q}^{(j)}(m)\mathbf{P}_{k,l}^{(q)}(m)$$

4. Repeat the previous steps for each iteration over k.

Figure 6(a) shows the overall system Bit Error Rate (BER) for different numbers of users. It also provides a comparison between the MMSE joint interference canceller/equalizer presented in this paper and the zero forcing interference canceller/MMSE equalizers of [6]–[8]. It is seen that adding one receive antenna does not only allow us to add one more user to the system but also increases the overall performance of the system.

In the second scenario we simulate the performance of the adaptive receiver. In this case, the channel impulse response does not need to be known at the receiver anymore. Moreover, no channel estimation is required at the receiver. The receiver uses a few blocks of known data for training and then switches to the decision directed mode. The learning curves of the adaptive receiver are shown in Figure 6(b). In this simulations, we assumed a Doppler frequency of 1Hz and SNR = 20dB. The curve shows the mean square error (MSE) of the adaptive receiver when the system has 2 users and 8 users, respectively. Figure 6(b) shows that as the number of users in the system increases and, subsequently, the number of receive antennas, the MSE decreases at the expense of a slower convergence.

We also simulate the BER performance of the adaptive receiver. Figure 6(c) shows the BER as a function of the average SNR per bit (E_b/N_0) at two different Doppler frequencies ($f_d = 1$Hz and $f_d = 20$Hz). It is seen from the curves that the performance of the adaptive receiver is similar to that of the MMSE receiver shown in Figure 6(a). However, as the Doppler frequency increases, the performance degradation due to the channel fast variations has to be overcome by adding retraining

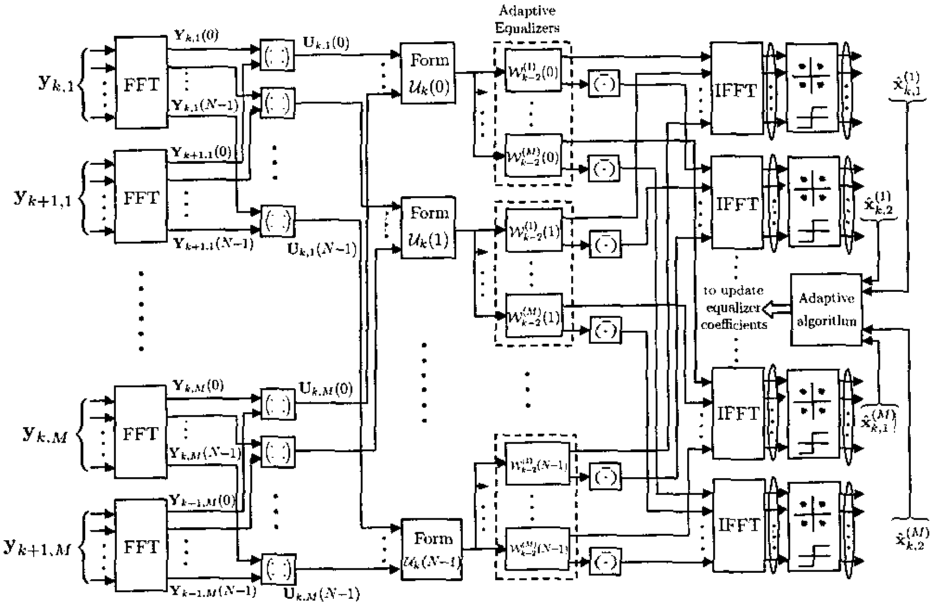

Fig. 5: An adaptive receiver structure for an M-user system with $2M$-transmit and M-receive antennas.

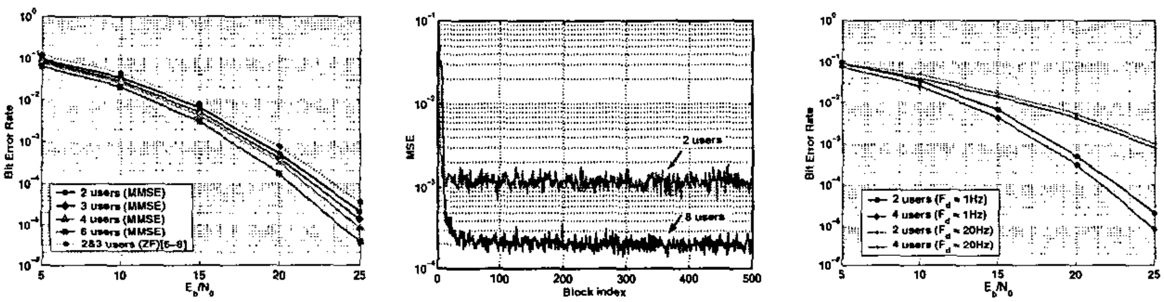

(a) BER performance of the per-symbol MMSE receiver for different number of users.

(b) Learning curves of the RLS adaptive receiver for different number of users.

(c) BER performance of the RLS adaptive receiver.

Fig. 6: Simulation results.

blocks. More discussions on this issue could be found in [8].

V. Conclusion

In this paper we developed efficient receiver structures for multi-user systems employing frequency-domain single-carrier space-time block codes over frequency selective fading channels. We exploited the structure of the STBC to show that the complexity of the receiver becomes similar to that of the receiver of an Alamouti STBC over flat fading channels. We also indicated that adding one receive antenna for each co-channel interfering user not only suppresses interference but also improves the system performance over the single user case.

References

[1] G. J. Foschini and M. J. Gans, "On limits of wireless communications in a fading environment when using multiple antennas," *Wireless Personal Communications*, vol. 40, no. 6, pp. 311–335, Aug. 1998.

[2] S. Alamouti, "A simple transmit diversity technique for wireless communications," *IEEE J. Select. Areas Commun.*, vol. 16, no. 8, pp. 1451–1458, Oct. 1998.

[3] V. Tarokh, H. Jafrakhani, and A. R. Calderbank, "Space-time block codes from orthogonal designs," *IEEE Trans. Inform. Theory*, vol. 45, pp. 1456–1467, July 1999.

[4] E. Lindskog and A. Paulraj, "A transmit diversity scheme for delay spread channels," *Proc. ICC*, New Orleans, LA, pp. 307–311, June 2000.

[5] N. Al-Dhahir, "Single-carrier frequency-domain equalization for space-time block-coded transmissions over frequency-selective fading channels," *IEEE Commun. Lett.*, vol. 5, no. 7, pp. 304–306, July 2001.

[6] A. Stamoulis, N. Al-Dhahir, and A. R. Calderbank, "Further results on interference cancellation and space-time block codes," in *Proc. 35th Asilomar Conference on Signals, Systems and Computers*, Pacific Grove, CA, pp. 257–261, Nov. 2001.

[7] W. M. Younis, A. H. Sayed, and N. Al-Dhahir, "Adaptive frequency-domain joint equalization and interference cancellation for multi-user space-time block-coded systems," *Proc. ICC*, Anchorage, AK, pp. 3230 –3235, May 2003.

[8] ——, "Efficient adaptive receivers for joint equalization and interference cancellation in multi-user space-time block-coded systems," *IEEE Trans. Signal Processing*, vol. 51, no. 11, pp. 2849-2862, Nov. 2003.

[9] A. F. Naguib, "Combined interference suppression and frequency domain equalization for space-time block coded transmission," in *Proc. ICC*, Anchorage, AK, pp. 3261 –3266, May 2003.

[10] A. Oppenheim and R. Schafer, *Discrete Time Signal Processing*. NJ: Prentice Hall, 1989.

[11] A. H. Sayed, *Fundamentals of Adaptive Filtering*. NY: Wiley, 2003.